Method of Effective Ellipses for Digital Image Analysis of Size, Shape, Orientation, and Interparticle Distances in Polymer Blends: Application to a Study of Polyamide 6/Polysulfone Reactive Blending

Grigori M. Sigalov,† Joel Ibuki, Tsuneo Chiba, and Takashi Inoue*

Department of Organic and Polymeric Materials, Tokyo Institute of Technology, 2-12-1 Ookayama, Meguro-ku, Tokyo 152, Japan

Received June 10, 1997; Revised Manuscript Received October 13, 1997[⊗]

ABSTRACT: A new DIA (digital image analysis) oriented method for the polymer blend morphology analysis was developed. The particles seen on SEM (scanning electron microscopy) pictures of the two-phase blends are considered as ellipses rather than circles, so that to be dealt with are their asphericity and orientation. Moreover, replacement of the particle patterns of complex shape by effective ellipses significantly simplifies calculation of such characteristics of the blend morphology as center-to-center (CC) and surface-to-surface (SS) interparticle distance distributions. With the help of a DIA computer program designed on the basis of the proposed algorithms, a series of SEM pictures for polyamide 6/polysulfone blends were analyzed, and new regularities of the blend morphology evolution during mixing were revealed. The changes in the CC and SS interparticle distance distributions, particle orientation distribution, and particle asphericity−size correlation were first characterized quantitatively.

Introduction

Among the methods of morphology analysis of two-phase polymer blends consisting of particles dispersed in a continuous matrix, most powerful are light scattering (LS) and electron microscopy (EM). While LS is a much more fast and less expensive tool than EM, a few morphology characteristics may be extracted unambiguously from LS data. For an ensemble of spherical particles with a known type of particle size distribution (PSD), the average particle size and PSD width, as well as the correlation length of the spatial distribution, may be found.[1,2] The shape of monodispersed ellipsoidal particles may be obtained together with their equivalent diameter from depolarized LS data treated with the help of the T-matrix (extended-boundary-conditions) method.[3,4] However, this does not work well when the distributions of particle size and shape are not very narrow. Last but not least, the multiple scattering which takes place at higher particle number densities makes the LS data virtually intractable. An attempt to overcome this obstacle restricted to the case of double scattering was reported recently.[5] Among other scattering techniques, neutron diffraction[6] and wide-angle X-ray scattering[7] have been used to investigate the orientation of crystalline nonspherical domains within a glassy matrix.

In contrast to the scattering methods which yield data about certain bulk-averaged characteristics of a material, the binarized EM pictures contain too much information which often allows us to describe in detail particular particles, interfaces, or small domains of the material but not the material as a whole. It is not trivial to derive the parameters characterizing the material's bulk properties and structure from local (pixel-scale) data. Thus, the problem of design of adequate algorithms and computer programs for digital image analysis (DIA) arises. Recent studies have shown[8] that even calculation of the number of particles on a certain EM picture is not a simple problem, and different approaches yield different figures. Much more involved is the determination of such structural characteristics as the interparticle distances and their distributions. Correct measurement of these parameters is necessary for establishing the processing conditions−morphology and morphology−properties correspondences, i.e., for the design of materials with prescribed mechanical, optical, and other characteristics. In particular, the surface-to-surface interparticle distance was found to be a critical parameter responsible for the fracture mechanism and toughness of brittle polymer matrices filled with rubber particles.[9] Thus, the development of robust methods of characterization of dispersed particles/matrix polymer blends is important both for academic research and technological purposes.

DIA methods have been used for characterization of droplet patterns in polymer blends.[10] The nearest-neighbor center-to-center distances and effective coordination number (number of cell sides of corresponding Voronoi polygons) of dispersed particles were measured. In a DIA study of surface structure development in swelling gels[11] the distribution of cell boundary orientations was calculated with the help of a 2-dimensional spatial Fourier transform. However, the shape and orientation of individual particles, as well as the surface-to-surface interparticle distances, have not been touched yet.

The aim of this paper is to introduce a new method of morphology analysis which would enable us to correctly take into account particle asphericity and orientation. Moreover, the approach presented below significantly simplifies calculation of such important structural characteristics of polymer blends as center-to-center and surface-to-surface interparticle distances, particle section perimeters, and coordination numbers. Our approach is based on replacement of the particle section patterns, which are generally rather complex, by *effective ellipses* rather than circles, which are usually

* To whom correspondence should be addressed.
† Permanent address: Institute of Chemical Physics in Chernogolovka, Russian Academy of Sciences, Chernogolovka, 141700 Moscow region, Russia.
⊗ Abstract published in *Advance ACS Abstracts,* November 15, 1997.

S0024-9297(97)00838-3 CCC: $14.00

adopted by conventional methods. This allows us to take into account the real shape (asphericity) of the particles, which is known to influence—sometimes crucially—such properties of composite materials as elastic moduli,[12] thermal expansion coefficient,[13] light-scattering characteristics,[14,15] magnetic susceptibility,[16] and so on.

On the basis of the algorithms developed, a computer program for DIA was designed. This particular program is restricted to the case of scanning electron microscopy (SEM) pictures or other pictures without overlapping of particle projections and needs preliminary sharpening of the particle boundaries by other tools (conventional software of this kind is available[17]). Meanwhile, the method itself is valid for any kind of dispersed particles/matrix type of blend morphology.

In order to make the presentation of the method of effective ellipses most clear and free of possible artifacts, we have ignored in this study the difference between the original sizes of real three-dimensional particles and their two-dimensional sections. This may be taken into account in further works with the help of stereological methods.[18]

The paper is organized as follows. The general problem of particles/matrix type image analysis is formulated in the next section; then the equations lying as the basis of the method of effective ellipses are derived. Further, an example of an application of this approach to analysis of SEM pictures of the blends prepared by reactive processing is given. Finally, conclusions are drawn.

General Problem of Digital Image Analysis of the Dispersed Phase Particles

The most general problem of morphology study by DIA for a polymer blend section analysis is to recognize the particles of the dispersed phase and to calculate the following: (1) their number, N; (2) the area of each particle section, S_n; (3) the perimeter of each particle section, P_n; (4) the orientation angle of each particle, α_n; (5) some parameter(s) (to be defined) which would characterize the particle shape, ζ_n; (6) the center-to-center (CC) interparticle distances, R_{mn}; (7) the surface-to-surface (SS) interparticle distances, r_{mn}; and (8) the coordination number for each particle, C_n, where $n = 1, ..., N$ is the particle number. Another problem is to analyze the distributions of the parameters C_n, S_n, P_n, α_n, ζ_n, R_{mn}, and r_{mn}, as well as the appropriate correlations between them.

Usually only a part of these subproblems is solved. Calculation of the above parameters must be preceded by proper definition of such notions as particle center, orientation angle, shape parameter(s), and particle neighbors. Some of these notions are rather involved to be defined for an arbitrary nonregular system of particles of nonspherical shape, while others can be easily defined but in practice possible correct definitions lead to serious computational difficulties.

Below we introduce an approximate approach which would make possible overcoming the above obstacles.

Method of Effective Ellipses: The Basic Equations

The image to be analyzed by computer is a set of pixels, p_{ij}, where i and j are discrete Cartesian coordinates. Below we suppose the binarized picture to be a black-and-white image, $p_{ij} = 1$ corresponding to particle sections (black) and $p_{ij} = 0$ to the matrix phase (white)

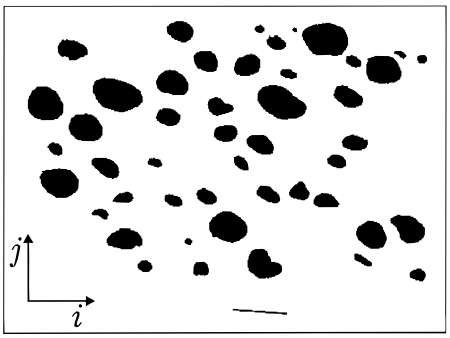

Figure 1. Typical example of a binarized black-and-white SEM picture (nonreactive PA6/PSU 70/30 blend, mixing time 2 min). The length of the scale bar is 5 μm.

(Figure 1). The algorithms or programs for transformation of the halftone gray image into a black-and-white image may be found elsewhere.[17] We use the dimensionless pixel units to express length and area values. If the scale is given, transition to physical units is straightforward.

For a particular particle P the definitions of mass center coordinates and area are most straightforward:

$$i_0 = S^{-1}\sum_{i,j} ip_{ij}, \quad j_0 = S^{-1}\sum_{i,j} jp_{ij} \tag{1}$$

where the area S is simply the number of pixels making up P,

$$S = \sum_{i,j} p_{ij}, \quad p_{ij} = \begin{cases} 1, & (i,j) \in \mathrm{P} \\ 0, & (i,j) \notin \mathrm{P} \end{cases} \tag{2}$$

Note that i_0 and j_0 may have fractional values, while i and j are integers.

Let us approximate the particle P by an ellipse E such that

(1) the mass center coordinates of P and E coincide, (2) the area of E is same as that of P, and (3) the mass distribution in P and E is similar, i.e., the moments of inertia of P and E coincide. In the local coordination system with the origin in the particle mass center, $x = i - i_0$, $y = j - j_0$, the moments of inertia relative to the coordination axes are defined as[19]

$$I_x = (\sum_{i,j} j^2 p_{ij}) - j_0^2 S, \quad I_y = (\sum_{i,j} i^2 p_{ij}) - i_0^2 S,$$
$$I_{xy} = (\sum_{i,j} ijp_{ij}) - i_0 j_0 S \tag{3}$$

Let (ξ, η) be a system of coordinates obtained from (x, y) by rotation to angle α counterclockwise (Figure 2). Then

$$\xi = x\cos\alpha + y\sin\alpha, \quad \eta = -x\sin\alpha + y\cos\alpha \tag{4}$$

therefore

$$I_\xi = I_x\cos^2\alpha + I_{xy}\sin 2\alpha + I_y\sin^2\alpha \tag{5}$$

$$I_\eta = I_x\sin^2\alpha - I_{xy}\sin 2\alpha + I_y\cos^2\alpha \tag{6}$$

$$I_{\xi\eta} = \frac{1}{2}(I_y - I_x)\sin 2\alpha + I_{xy}\cos 2\alpha \tag{7}$$

The principal axes of a plain figure are defined by the condition $I_{\xi\eta} = 0$; therefore, the angle of transformation

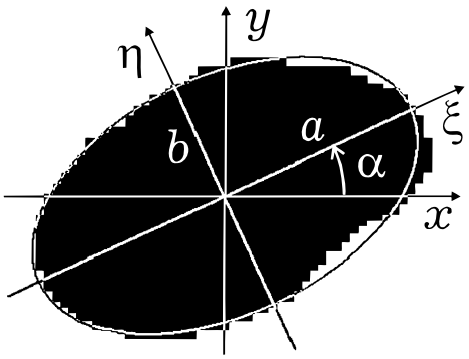

Figure 2. Binarized particle section pattern showing pixel quantization (exaggerated) and its effective ellipse (contrast contour).

to the principal axes is derived from eq 7 as

$$\alpha = \frac{1}{2}\arctan\frac{2I_{xy}}{I_x - I_y} \tag{8}$$

The angle α characterizes the particle orientation. Now I_ξ and I_η are given by eqs 5 and 6 with α from eq 8. Since we are free to choose one of the two principal axes as the particle orientation direction and to add $\pm\pi$ to α, we define it below so that $a \geq b$ and $-\pi/2 < \alpha \leq \pi/2$.

For an ellipse with semiaxes a and b along the ξ- and η-axes, respectively,

$$S = \pi ab, \quad I_\xi = b^2S/4, \quad I_\eta = a^2S/4 \tag{9}$$

For a particle P of general shape the conditions in eq 9 cannot be satisfied simultaneously, but we can keep the aspect ratio and define the semiaxes of the effective ellipse corresponding to P by the relationships $S = \pi ab$ and $a/b = (I_\eta/I_\xi)^{1/2}$. Substituting S from eq 2 and I_ξ, I_η from eqs 5 and 6 with α from eq 8, we obtain

$$a = \sqrt{\pi^{-1}S(I_\eta/I_\xi)}^{1/2}, \quad b = S/\pi a \tag{10}$$

The particle asphericity may be characterized by a parameter introduced as follows:

$$\zeta = a/b - 1 \tag{11}$$

And the deflection of the real shape of particle P from the corresponding ellipse E (the relative approximation error of the proposed method) may be characterized by the parameter

$$\mu = \frac{I_P - I_E}{I_E} = 4\frac{I_\xi + I_\eta}{\pi ab(a^2 + b^2)} - 1 = 4\pi\frac{\sqrt{I_\xi I_\eta}}{S^2} - 1 \tag{12}$$

where I_P and I_E are the central moments of inertia of the particle and the ellipse, while I_ξ and I_η are the principal axial moments of particle P, as before.

Now for many purposes we can consider effective ellipses instead of real particles. Thus, from the viewpoint of computer DIA, for every particle we have to store only five values (i_0, j_0, a, b, α) instead of S pairs of (i, j) coordinates. Application of this approach for calculation of miscellaneous morphology parameters is described below.

Particle Perimeter. The perimeter of a particle may be found now approximately as the perimeter of the corresponding ellipse[20]

$$P = 4a\mathrm{E}(\epsilon) = 4a\int_0^{\pi/2}\sqrt{1 - \epsilon^2\sin^2\psi}\,\mathrm{d}\psi \tag{13}$$

where E(ϵ) is the Legendre's complete elliptic integral of the second kind and ϵ is the ellipse eccentricity, $\epsilon = (1 - b^2/a^2)^{1/2} < 1$. A series expansion version of eq 13 may be used in numerical calculations,

$$P = 2\pi a\left[1 - \left(\frac{1}{2}\right)^2\frac{\epsilon^2}{1} - \left(\frac{1\cdot3}{2\cdot4}\right)^2\frac{\epsilon^4}{3} - \left(\frac{1\cdot3\cdot5}{2\cdot4\cdot6}\right)^2\frac{\epsilon^6}{5} - \ldots\right] \tag{14}$$

Interparticle Distances. The center-to-center (CC) interparticle distances R_{mn} between particles P_m and P_n can be easily obtained as $R_{mn} = [(i_{0m} - i_{0n})^2 + (j_{0m} - j_{0n})^2]^{1/2}$, where (i_{0k}, j_{0k}) are the coordinates of the mass center of particle P_k found according to eq 1.

To find the surface-to-surface (SS) interparticle distances r_{mn}, consider two effective ellipses E_m and E_n (Figure 3). It is easy to find that

$$r_{mn} = R_{mn} - \rho_m - \rho_n, \quad \rho_k = \left(\frac{\cos^2\beta_k}{a^2} + \frac{\sin^2\beta_k}{b^2}\right)^{-1/2} \tag{15}$$

where $R_{mn} = |\mathrm{AD}|$ and $r_{mn} = |\mathrm{BC}|$ are the CC and SS distances, respectively, $\rho_m = |\mathrm{AB}|$, and $\rho_n = |\mathrm{CD}|$. The angles β_k are defined as

$$\beta_m = \gamma_{mn} - \alpha_m, \quad \beta_n = \gamma_{mn} + \pi - \alpha_n, \quad \gamma_{mn} = \arctan\frac{j_{0n} - j_{0m}}{i_{0n} - i_{0m}} \tag{16}$$

Definition of Neighbors and Coordination Number. Approach of effective ellipses makes it possible to define unambiguously the notion of neighbors and coordination number for the given particle (Figure 4). Let us draw the tangent lines from the center of ellipse E_1 to all other ellipses. If an ellipse is not shaded by any other one (such is E_2 and E_4 in our example), it is called a *(full) neighbor* to ellipse E_1. Partially shaded ellipses, like E_3, may be called *partial neighbors* of E_1, while totally shaded ellipses, like E_5, are not neighbors at all. The number of full neighbors of the given particle is then called its coordination number, C. If needed for a specific purpose, the partial neighbors may also be taken into account.

To make possible quantitative analysis of this matter, let us calculate the angles and lengths of the tangent lines drawn from the center $A = (i_{0m}, j_{0m})$ of an ellipse E_m to the ellipse E_n with center $C = (i_{0n}, j_{0n})$, orientation α, and principal semiaxes a and b (Figure 5). With the help of simple but lengthy geometric transformations it can be shown that in this case

$$\tan\phi_1 = \tan\beta \times \frac{p - q^{-1}}{p + q}, \quad \tan\phi_2 = \tan\beta \times \frac{p + q^{-1}}{p - q} \tag{17}$$

$$r_1 = |\mathrm{AB}| = \frac{pR}{p^2 + 1}\sqrt{(p + q)^2\cos^2\beta + (p - q^{-1})^2\sin^2\beta} \tag{18}$$

$$r_2 = |\mathrm{AD}| = \frac{pR}{p^2 + 1}\sqrt{(p - q)^2\cos^2\beta + (p + q^{-1})^2\sin^2\beta} \tag{19}$$

where β is given by either of eqs 16 and

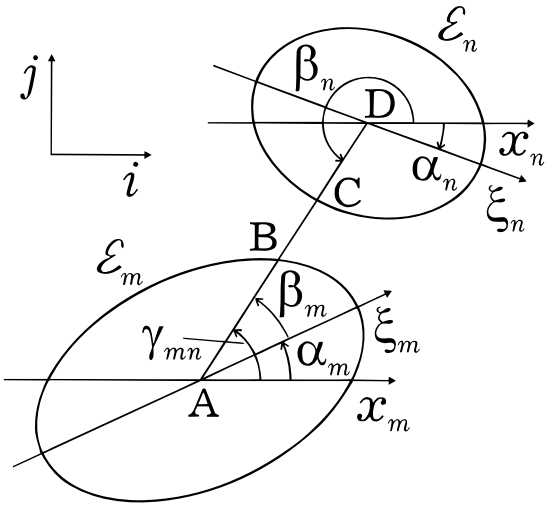

Figure 3. On the definition of CC and SS interparticle distances. Coordinates of the ellipses centers, *A* and *D*, are (i_{0m}, j_{0m}) and (i_{0n}, j_{0n}), respectively. x_m and x_n are the axes of local (x, y) coordination systems; ξ_m and ξ_n are the axes of local (ξ, η) coordination systems. Note that x_m and x_n are always parallel to each other while ξ_m and ξ_n are not, in the general case.

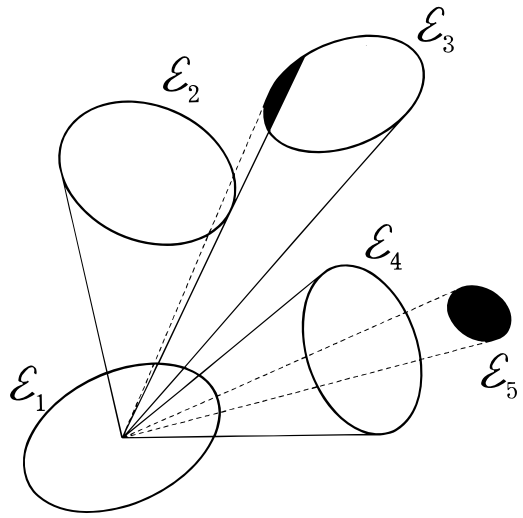

Figure 4. On the definition of neighbors and coordination number.

$$p = \sqrt{R^2\left(\frac{\cos^2\beta}{a^2} + \frac{\sin^2\beta}{b^2}\right) - 1}, \quad q = \frac{a}{b}\tan\beta \qquad (20)$$

Now the tangent angles are easily obtained as $\psi_i = \pi - \alpha - \phi_i$. Then we proceed as follows. For every particle P_k we calculate the angles and lengths for tangent lines plotted from its center to all other particles. Comparing the angles and lengths for all pairs (P_m, P_n), m, $n \neq k$, we find out which particles are shaded (entirely or partially) or not shaded and, therefore, which of them are full or partial neighbors of P_k. Information obtained in this way may be used, e.g., to establish a criterion for the single/multiple light-scattering conditions.

Study of PA6/PSU Blends Morphology with the Method of Effective Ellipses

Experimental Section. The method of effective ellipses was applied to the investigation of morphology development in polyamide/polysulfone blends at reactive blending. The polyamide used was a commercial polyamide 6 (PA6) supplied by BASF AG (Ultramid B3; M_n = 13 000, M_w = 25 000). Two polysulfone (PSU) specimens were used: one was a nonreactive PSU (M_n = 5300, M_w = 21 700), and the other was a PSU grafted with 1.35 wt % maleic anhydride groups, PSU*g*MAH (M_n = 7540, M_w = 19 266). The reactive PSU was prepared by Dr. M. Weber, BASF AG. The PSU and PA6 were melt-mixed at a 20/80 weight ratio in a miniature mixer, Mini-Max molder (Custom Scientific Instruments, model CS-183MMX) at 260 °C. The rotor speed of 100 rpm was kept constant for all blends. At various mixing times the rotor was lifted and about 40 mg of mixed melt was sampled and quenched immediately in water to freeze the two-phase structure. Samples of the blend were picked up after 1, 2, 4, 6, and 8 min of mixing.

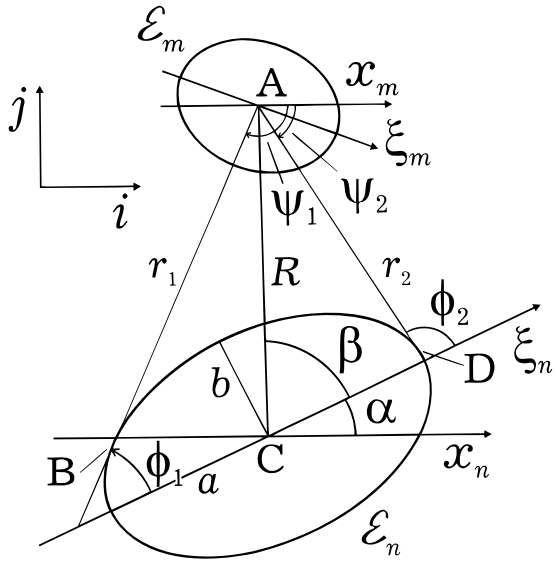

Figure 5. On calculation of tangent lines' angles and lengths.

The quenched specimens taken at each mixing time were cryomicrotomed at −15 °C with a ultramicrotome (Reichert Ultracut-Nissei) using a glass knife. A flat and mirror-like surface was created, and then the blend was immersed in tetrahydrofuran, THF (good solvent for PSU). Thus the PSU phase was selectively removed, and the holes left were observed with a scanning electron microscope (model JSM-T220, JEOL Ltd.) at the accelerating voltage of 15 keV. The SEM pictures were digitized using a scanner EPSON GT-50.

Software Description. Digitized pictures obtained for each sample were treated with the help of a custom-designed computer program based on the method of effective ellipses. The program for image recognition and analysis was developed on an IBM PC computer in the Turbo C programming language. The image files to be analyzed by the program had to be in the PCX format. The size of the images obtained from the scanner was 512 pixels × 512 pixels.

A special subroutine was developed to recognize the scale bar present on SEM pictures and calculate its length (in pixels) irrespective of its orientation and shape perfection. The accuracy of this algorithm virtually reached the theoretical limit of $^1/_2$ pixel. The physical length (in micrometers) of the scale bar had to be specified in a configuration file read by the program. Thus, the physical dimensions of the image and particles were calculated.

To recognize the individual particles, the image is scanned along the rows to find the boundaries of the black domains (particles). For the *i*th row this yields a

Table 1. Summary of SEM Pictures Analyzed

image code[a]	t,[b] min	N[c]	$\bar{S}$,[d] μm^2	ΔS,[d] μm^2
N103	1	100	8.562	15.127
N107	2	47	3.419	2.770
N108	2	87	5.121	5.245
N112	4	50	1.574	1.191
N115	6	41	2.290	1.169
N116	6	36	2.630	1.092
N120	8	53	1.979	0.915
R827	1	133	1.380	2.822
R830	2	159	0.194	0.245
R832	4	146	0.144	0.167
R838	6	125	0.0616	0.0409
R835	8	166	0.0747	0.0450

[a] N and R in image codes stand for nonreactive and reactive systems. [b] t is the mixing time. [c] N is the number of particles present on the given picture. [d] $\bar{S}$ and ΔS are their average area and its standard deviation.

number of pairs (t^i_{1k}, t^i_{2k}), where t^i_{1k} and t^i_{2k} are the positions (j−coordinates) of the leftmost and rightmost pixels of the kth black domain in the ith row. Then the data for two adjacent rows are compared. If (t^i_{1k}, t^i_{2k}) has a nonzero overlap with ($t^{i+1}_{1k'}$, $t^{i+1}_{2k'}$) for some k and k', then it is concluded that these domains belong to the same particle. A special procedure takes care of nonconvex and even nonsimply connected patterns. As a result, all the pairs (t^i_{1k}, t^i_{2k}) for every individual particle are found. Every particle consists of pixels p_{ij} such that $t^i_{1k} \le j \le t^i_{2k}$ for all i and $k(i)$ corresponding to the given particle. Now it is easy to proceed to the steps described by eqs 1−3, 8, and so on. To be sure that the particles and the scale bar have been recognized correctly, a subroutine created an auxiliary image file with all particles painted as individual colors and the scale bar left black. This made possible easy visual control of the recognition.

Data Analysis and Discussion. We have analyzed seven SEM pictures for nonreactive PA6 PSU blends and five pictures for reactive PA6/PSU blends. Table 1 summarizes the primary data for each picture. One can see that the distribution of size is initially (t = 1 min) very broad and that it becomes more narrow during mixing. The changes in the particle size distributions for nonreactive and reactive systems are visualized by log−normal plots (Figure 6) of distributions of the particle effective diameter, $D = 2(S/\pi)^{1/2}$. In most cases the plots are seen to fit well enough the log−normal distribution. With the coordinates used in Figure 6, the mean for every time corresponds to 50% of cumulative probability, and the distribution width is inversely proportional to the plot slope.

For each individual particle on each picture the values i_0, j_0, S, α, a, b, ζ, P, μ, and C have been calculated. Also for each pair of neighboring particles on a given picture the interparticle distances R_{mn} and r_{mn} were found. Below we present and discuss part of these data which often cannot be obtained by conventional methods.

Interparticle Distances. It was shown by Wu[9] that the sharp transition of rubber-toughened materials from brittle to tough mode of fracture is governed by the surface-to-surface (SS) distances between rubber particles. In the interparticle distance model of impact fracture proposed by Wu, the rubber particles are assumed to be spherical, of the same diameter d, and arranged in a cubic lattice. The number-average particle diameter d_n determined from SEM pictures was employed as the model parameter d to compare theory

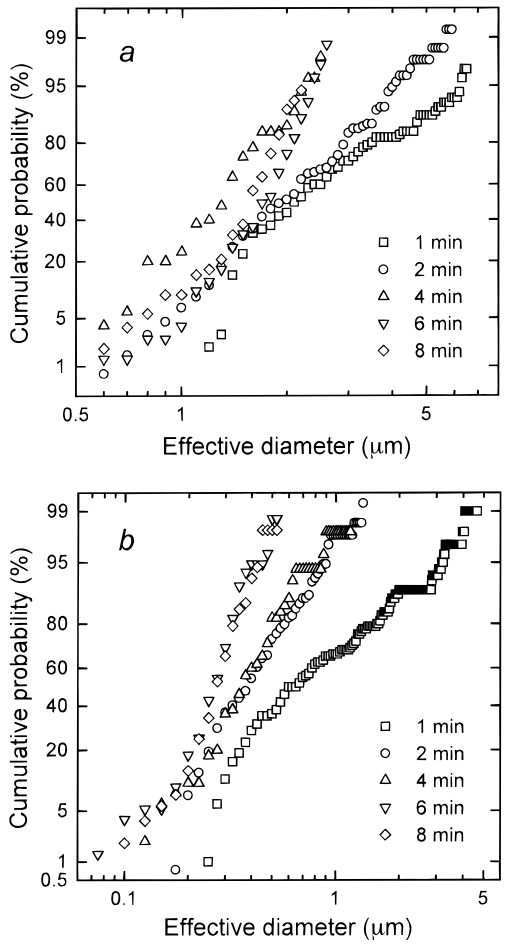

Figure 6. Log−normal plots of particle effective diameter distributions at different times of mixing for (a) nonreactive and (b) reactive PA6/PSU blends.

and experiment. Although the actual distribution of particle sizes was neglected, this model allowed Wu to achieve good qualitative correspondence with experimental data. Once a fitting parameter, the critical SS interparticle distance T_c, was introduced, quantitative agreement was obtained. However, the *actual* SS interparticle distances have not been measured directly to be compared with T_c, which was, in fact, a kind of best-fit parameter. Their numerical values may be expected to differ, since the geometry of a real material differs significantly from the simple cubic lattice.

It is natural to suggest that the impact behavior of the polymer blend is determined not only by average SS interparticle distance but rather by its distribution, especially by the short-distance part of the distribution (the long-distance "tail" may not influence essentially the fracture mode). The coordination number C is also of a great importance. It is clear that even for ideal models like that by Wu, T_c must depend on the lattice type, each type being characterized by a specific coordination number.

To demonstrate how the interparticle distance may be analyzed for a real material, we calculated its full distributions for the series of SEM pictures of PA6/PSU blends described in Table 1. Figure 7 shows a typical histogram of SS and CC interparticle distances' distributions. CC distances may also be used for discrimination of the fracture mechanisms, as discussed by Matsuo *et al.*[21] Note that the most essential difference appears at small distances. Even more vivid representation of the distribution is given by a plot in log−normal

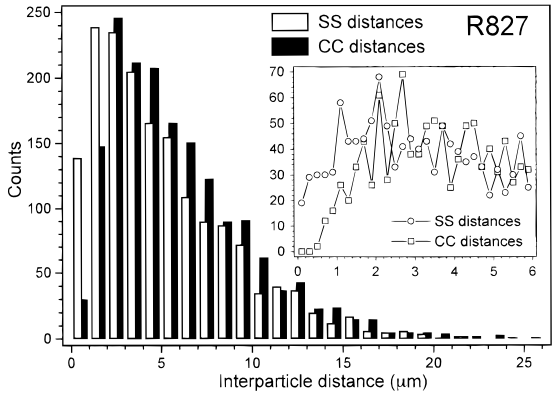

Figure 7. Histogram of SS and CC interparticle distances' distribution for the image R827 (reactive PA6/PSU system, 1 min of mixing). The inset shows the same distribution in more detail for short distances.

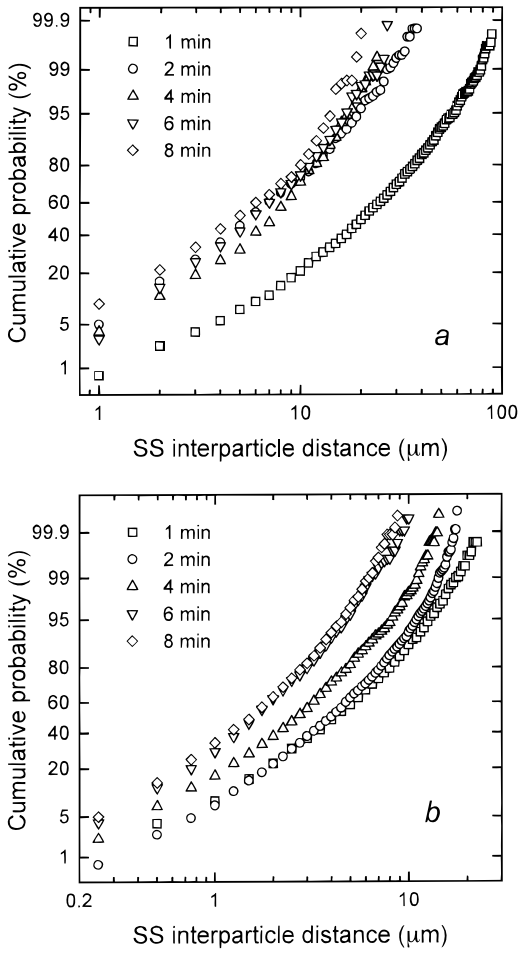

Figure 8. Log−normal plots of SS interparticle distances' distribution at different times of mixing for (a) nonreactive and (b) reactive PA6/PSU blends.

coordinates. The changes of the SS interparticle distances' distribution during the mixing of nonreactive and reactive blends are shown by Figure 8.

Analysis of variation with mixing time of the surface-to-surface interparticle distance distribution (SS IPDD) and the particle size distribution (PSD) has shown that the changes in the SS IPDD and the PSD are not simultaneous or simply correlated. For the nonreactive system, the initial (from 1 to 2 min) considerable change in the SS IPDD is accompanied by only a slight change in the PSD, while a further (2−4 min) jump in the PSD corresponds to a minor variation in the SS IPDD.

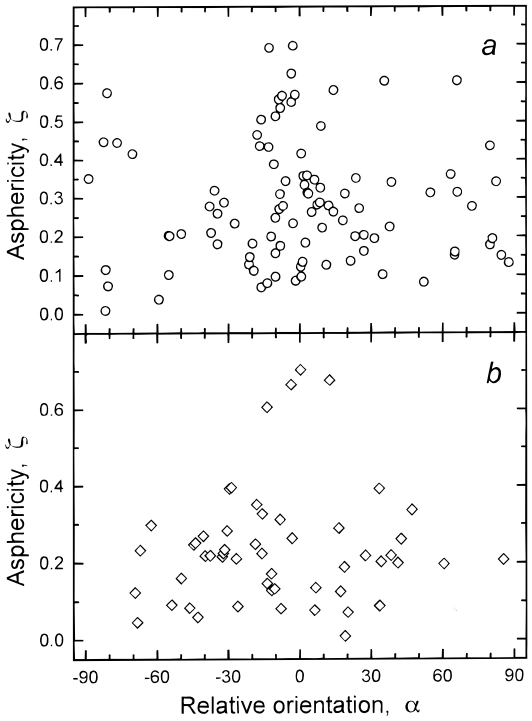

Figure 9. Plot of particles' asphericity vs their relative orientation (definition in the text) for the nonreactive PA6/PSU blend after (a) 1 min and (b) 8 min of mixing.

Although the average particle size does not show a clear tendency to further decrease after 8 min of mixing, consideration of SS IPDD and PSD plots allows us to suggest that the structure formation in the nonreactive blend is not yet finished at this moment.

A different behavior is observed with the reactive PA6/PSU*g*MAH system. In the first stage of mixing (1−2 min) the change in the PSD is abrupt while only the far-distance part of the SS IPDD is changed noticeably. Then (2−4 min) only the short- and far-distance tails of the PSD change, while the whole SS IPDD curve is essentially shifted to smaller distances. Next (4−6 min), the change in the PSD and the SS IPDD is comparable, although the width (variation) of the PSD decreases to a greater extent than that of the SS IPDD. Finally, virtually nothing changes between 6 and 8 min. It may be argued that in an industrial process mixing may be stopped after 6 min, since the asymptotic properties—at least those which are defined by the PSD and the SS IPDD[9]—are already reached.

Orientation of Particles during Mixing. The particles dispersed in a viscous media subject to shear or complex flow tend to become oriented along the flow line. This process is completed by chaotic rotation of particles due to their complex shape (in fact, even spherical particles are rotating in the flow) and flow fluctuations. As a result of such a competition, a distribution of orientation angles of dispersed particles arises. It is essential to know how to control this distribution which affects the mechanical,[22] optical,[23] and other properties of the final material.

Figures 9 and 10 illustrate the orientation process in nonreactive and reactive PA6/PSU blends, respectively, mixed for 1 and 8 min. The dimensionless asphericity parameter ζ for every particle was plotted against the orientation of this particle relative to an arbitrary axis (the latter was chosen to be close to the orientation of the most aspherical particle). It may be easily seen that the range of angles α is very broad (up to 180°) for

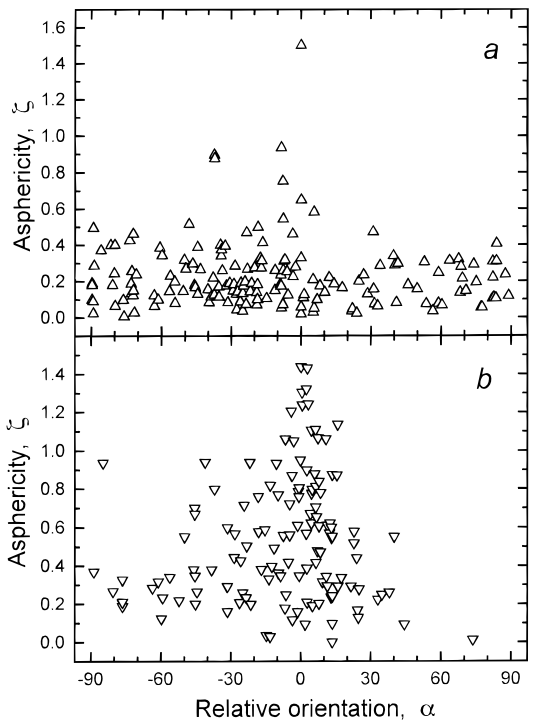

Figure 10. Same as in Figure 5, reactive PA6/PSU blend.

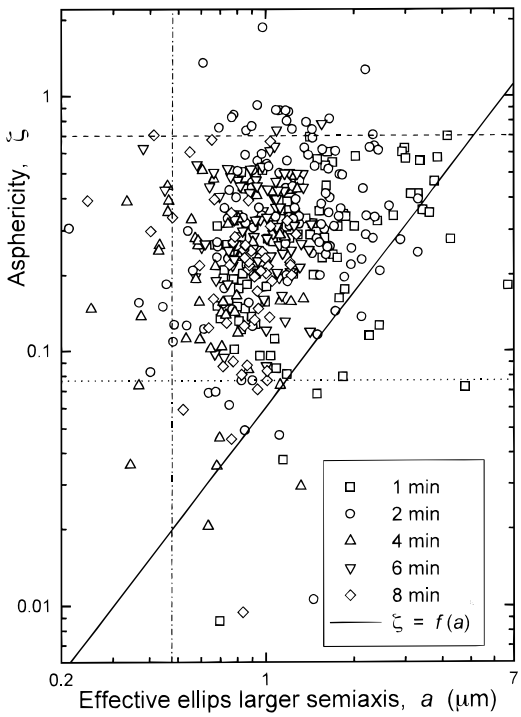

Figure 11. Particle asphericity−size correlation for the nonreactive PA6/PSU blend. The equation $\zeta = f(a)$ for the lower boundary is given in the text.

nearly spherical particles, as expected. The more elongated is a particle, the more narrow is the range of its probable orientation angles. During mixing the OAD becomes generally more narrow, in particular for nearly spherical particles. It may also be claimed that the OAD is more regular for the reactive system than for the nonreactive one. More detailed analysis, in particular concerning the effect of the compatibilization and mixing time, may be made on the basis of a physical model which would describe quantitatively the flow in the mixer, fractionation and dispersion of particles in the shear flow, and the statistics of final orientation of particles depending on their shape and size. Although such a theory is still lacking, some recent papers[24,25] may be considered as essential contributions to it.

Shape Relaxation of Dispersed Particles. Since the initial size of the PSU pellets loaded to the mixer was roughly 1 mm and the final size of PSU domains was of the order of 1 μm, all the particles that we observe on SEM pictures have been formed via breakup of larger particles. Therefore, the shape of each particle at the moment of its birth was irregular. Until both phases are solidified, the particle evolves toward more regular shape to minimize the interfacial energy. This process in counteracted by perturbation of the particle shape by shear tension due to the shear flow. Thus, information about the final particle shape distribution in suddenly frozen samples may throw light onto mixing and fragmentation mechanisms.

To characterize the process of shape relaxation of dispersed particles, we plotted the particle asphericity ζ against the particle size expressed by the larger semiaxis a of the corresponding effective ellipse. All the pairs (a, ζ) for particles from all the pictures for the given type of blend were collected to make a single plot in double-log coordinates. For the nonreactive system, 414 points in total formed Figure 11. The set of points has a visual boundary, though very loose. To determine this boundary more definitely, we plotted horizontal lines $\zeta = \zeta_1$ and $\zeta = \zeta_2$ such that 95% of the points lie below or over them and a vertical line $a = a_1$ such that 95% of the points lie to the right of this line. The boundary values found this way are $\zeta_1 = 0.70$, $\zeta_2 = 0.0766$, and $a_1 = 0.478$. The point set is also bound from the right and below by a curve which may be described by the equation $\zeta = (a/a_2)^n$, a_2 being of the same dimensionality as a. For a curve of this kind defined so that 95% of the points lie to the left and above it, the best fit is given by $a_2 = 6.5$ μm, $n = 1.5$.

For the reactive system, 729 points were collected together (Figure 12). The horizontal boundaries from above and below and the vertical leftmost boundary may be defined the same way. The sloping boundary from right and below is more sharp and may be fitted by the equation

$$\zeta = (a/a_0)^{n_1}/\sqrt{c + (a/a_0)^{n_1}} \qquad (21)$$

where a_0 has length dimensionality and n_1, n_2, and c are dimensionless. The curve in Figure 12 was plotted with the parameters $a_0 = 2.4$ μm, $n_1 = 2.5$, $n_2 = 3$, and $c = 0.001$. About 3% of the points lie below this curve. Of course, all the boundaries are not very sharp and therefore may also be described by slightly different empirical equations if those would be suggested by a phenomenological model of the process.

An explanation of such a behavior may be as follows. During mixing the particles are alternatively subject to shear stress and left to relax. The larger is a particle, the more it gets deformed during shearing and the less it recovers the spherical shape during "rest" time because of the relatively weaker influence of the interface. Indeed, the relaxation to the spherical shape is driven by the surface tension and hindered by the viscosity of the particle and the matrix. Interface effects dominate over bulk effects when the particle size is small enough, and vice versa.

Once the blend is quenched, the shape relaxation process is virtually frozen, and all particles remain less

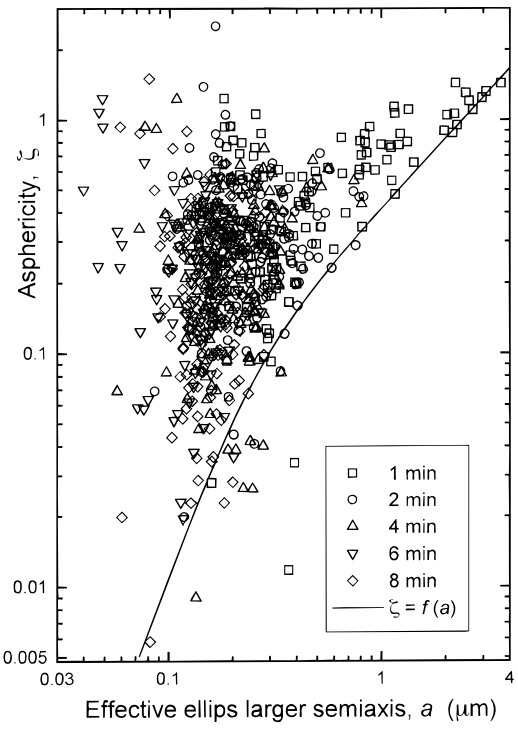

Figure 12. Same as in Figure 11, reactive PA6/PSU blend.

or more aspherical; the larger is a particle, the greater is its residual asphericity ζ. This explains qualitatively the existence and the character of the inclined lower boundary of the distribution $\zeta(a)$. The upper boundary appears most likely due to the breakup of very elongated particles. This phenomenon leads to limitation from above of the observed asphericity. A perfectly spherical shape may only be reached asymptotically, within infinitely large times. Since the specimens are quenched immediately after sampling, the asphericity parameter should not be less than a certain value corresponding to the lower horizontal boundary.

It might be expected that the formation of block copolymer in the reactive system would lead to a more aspherical shape of particles. However, a comparatively weak interface energy in the reactive system leads also to easier breakup of the particles, so that their sizes are, in general, smaller than in the nonreactive system. The overall effect is that the distributions in Figures 11 and 12 are similar and the upper boundary for asphericity is virtually the same, although in the case of a reactive system the distribution is essentially shifted to smaller particle sizes.

Naturally, the distribution $\zeta(a)$ is determined by the viscoelastic properties of both phases, the interfacial energy, the pattern of flow in the mixer, and other factors. The detailed quantitative theory of the particle shape formation needs particular consideration which is beyond our goals.

Conclusion

Investigation of the morphology of polymer blends with the help of electron microscopy requires DIA methods able to recognize particles of the dispersed phase and to analyze in most possible details their size, shape, orientation, and mutual position. Most existent methods and available computer programs based thereon allow only partial solution to this problem, since they often consider particles as spheres. This makes impossible the investigation of particle orientation and contributes erroneously to measurement of other parameters.

In this paper we have introduced and developed a new method of characterization of the size, shape, and orientation of a single particle. Its essence is in replacing of the real particle section pattern by an effective ellipse defined so that the area, mass center, and moments of inertia of the section are preserved. The method of effective ellipses simplifies the treatment of such structural characteristics of polymer blends as center-to-center and surface-to-surface interparticle distances and coordination number. All the aforementioned values may be calculated for every individual particle (or pair of particles, if applicable), so that their distributions may also be found.

The new method was applied to analysis of SEM pictures of two kinds of PA6/PSU blends. The evolution of the blend morphology during mixing was examined, and the differences in the behavior of reactive and nonreactive systems were revealed. In particular, the correlation between particle size and its residual asphericity was first characterized quantitatively.

It was also found that the evolution of the interparticle distance distribution is, to a certain extent, independent of the particle size reduction process. Since both these characteristics influence the mechanical properties (especially the fracture toughness) of the material, a possibility of more smart manipulation of these properties via control of the material structure arises.

The new method of the blend morphology analysis presented in this paper and the examples of its application to the study of morphology evolution during blending of two kinds of PA6/PSU systems provide an extensive empirical basis for the theoretical analysis of the processes involved as well as for the accurate quantitative control of the blend characteristics in technological applications.

Acknowledgment. The authors are grateful to the German Government, BMBF, for providing them a research fund (Project 03 N30283). We also appreciate the collaboration of Dr. Martin Weber and Dr. Eckhard Koch, BASF AG.

References and Notes

(1) van de Hulst, H. C. *Light Scattering by Small Particles*; Dover: New York, 1957.
(2) Bohren, C. F.; Huffman, D. R. *Absorption and Scattering of Light by Small Particles*; Wiley: New York, 1983.
(3) Quirantes Sierra, A.; Delgado Mora, A. V. *Appl. Opt.* **1995**, *34*, 6256.
(4) Barber, P. W.; Hill, S. C. *Light Scattering by Particles: Computational Methods*; World Scientific: Singapore, 1990.
(5) Tishkovets, V. P.; Litvinov, P. V. *Opt. Spektrosk.* **1996**, *81*, 319.
(6) Clarke, S. M.; Rennie, A. R.; Convert, P. *Europhys. Lett.* **1996**, *35*, 233.
(7) Suh, C. H.; White, J. L. *Polym. Eng. Sci.* **1996**, *36*, 2188.
(8) Nishi, T.; Ikehara, T. VAMAS Report No.26, **1997** ISSN 1016−2186.
(9) Wu, S. *Polymer* **1985**, *26*, 1855.
(10) Tanaka, H.; Hayashi, T.; Nishi, T. *J. Appl. Phys.* **1989**, *65*, 4480.
(11) Hayashi, T.; Tanaka, H.; Nishi, T.; Hirose, Y.; Amiya, T.; Tanaka, T. *J. Appl. Polym. Sci.: Appl. Polym. Symp.* **1989**, *44*, 195.
(12) Luo, J.; Stevens, R. *J. Appl. Phys.* **1996**, *79*, 9057.
(13) Luo, J.; Stevens, R. *J. Appl. Phys.* **1996**, *79*, 9047.
(14) Mishchenko, M. I. *J. Opt. Soc. Am. A* **1991**, *6*, 871.
(15) Mishchenko, M. I.; Travis, L. D. J. *Quant. Spectrosc. Radiat. Transfer* **1994**, *51*, 759.

(16) Mattei, J. L.; Laurent, P.; Minot, O.; Lefloch, M. *J. Magn. Magn. Mater.* **1996**, *160*, 23.
(17) Among others, there are public domain software: *ImageTool* (http://ddsdx.uthscsa.edu/dig/itdesc.html) and *NIH Image* (http://rsb.info.nih.gov/nih-image).
(18) Sato, E.; Kondo, N.; Wakai, F. *Philos. Mag. A* **1996**, *74*, 215.
(19) Becker, R. A. *Introduction to Theoretical Mechanics*; McGraw-Hill: New York, 1954.
(20) Korn, G. A.; Korn, T. M. *Mathematical Handbook for Scientists and Engineers*; McGraw-Hill: New York, 1961.
(21) Matsuo, M.; Wang, T. T.; Kwei, T. J. *J. Polym. Sci., A-2* **1972**, *10*, 1085.
(22) Massardier, V.; Maire, E.; Merle, P. *Mater. Sci. Eng. A* **1995**, *203*, 105.
(23) Ahn, J. S.; Kim, K. H.; Noh, T. W.; Riu, D. H.; Boo, K. H.; Kim, H. E. *Phys. Rev. B* **1995**, *52*, 15244.
(24) Buyevich, Y. A. *Chem. Eng. Sci.* **1996**, *51*, 635.
(25) Potanin, A. A.; Verkhusha, V. V.; Muller, V. M. *Colloid J.* **1996**, *58*, 355.

MA970838F